Spectroscopic Studies on Plastocyanin Single Crystals: A Detailed Electronic Structure Determination of the Blue Copper Active Site

K. W. Penfield, R. R. Gay, R. S. Himmelwright, N. C. Eickman, V. A. Norris, H. C. Freeman, and E. I. Solomon*

Contribution from the Department of Chemistry, Massachusetts Institute of Technology, Cambridge, Massachusetts 02139, and Department of Inorganic Chemistry, University of Sydney, Sydney 2006, Australia. *Received October 30, 1980*

Abstract: We report the results of polarized single-crystal optical and single-crystal EPR spectral studies and ligand field calculations on the X-ray crystallographically defined blue copper site in poplar plastocyanin. These studies have enabled us to correlate the electronic structure of the blue copper active site with its geometric structure. First, a fairly detailed interpretation of the ligand-to-copper charge-transfer spectrum is presented. The three dominant absorption bands at 13 350, 16 490, and and 17 870 cm^{-1} are proposed to be cysteine(Cys) $\rightarrow$ Cu $d_{x^2-y^2}$ charge-transfer transitions. These are related to the nature of the Cu–S(Cys) bond; in particular, the σ interaction results from a sulfur p_y orbital due to the 107° R–S–Cu bond angle. The relative contributions of the histidines (His) and methionine (Met) to the remaining weaker transitions at 21 390 and 23 340 cm^{-1} are also considered. The methionine is concluded to make at most a small contribution to the charge-transfer spectrum, due to the length of the Cu–S(Met) bond (2.9 Å) and the poor overlap of the methionine sulfur orbitals with the Cu $d_{x^2-y^2}$ orbital. Second, the determination of the approximate orientation of the g tensor with respect to the blue copper site is discussed. It is found that the angle between g_z and the long Cu–S(Met) bond is ~5° and the half-occupied $d_{x^2-y^2}$ orbital is oriented less than 15° above each of the remaining three ligands. Next, we present an iterative ligand field calculation of the blue copper site which utilizes initial parameters derived from model complexes. This calculation is used to determine an approximate energy level diagram and g tensor. The results indicate that the blue copper site in plastocyanin is best represented as having elongated C_{3v} symmetry with significant rhombic distortions. The major axis is associated with the long Cu–S(Met) bond, and the rhombic distortions originate from the differences between the ligand field contributions of the two histidine nitrogens and the cysteine sulfur. Finally, the results of this study are used to interpret some of the spectral differences among blue copper proteins in terms of possible structural differences in their copper sites.

I. Introduction

Achieving a detailed interpretation of the unique spectroscopic features of the blue copper site found in a variety of proteins and multicopper enzymes has been a major goal in the bioinorganic chemistry of copper. These unique spectral features include an extremely intense absorption band (ϵ ~3–5000 M^{-1} cm^{-1}) at ~600 nm, with weaker bands at lower and higher energy in the visible spectrum and an axial EPR signal ($g_{\parallel} \sim 2.23$, $g_{\perp} \sim 2.05$) with a small copper parallel hyperfine splitting ($A_{\parallel} < 63 \times 10^{-4}$ cm^{-1}).[1-3] The aim of earlier spectroscopic studies of the blue copper site was to ascertain the geometric structure of the site from its electronic spectral features. This was accomplished[4,5] through the extension of the observed optical spectrum into the near-infrared (IR) region by using the IR circular dichroism (CD) spectrometer developed by Stephens et al.[6] Three new electronic absorption bands corresponding to ligand field transitions were observed for plastocyanin at 11 200, 9000, and 5100 cm^{-1}. An interpretation of these new spectral features in terms of ligand field theory led to a number of predictions concerning the blue copper site. First, a ligand field calculation of changes in the d–d transitions in response to a distortion from a square-planar to a tetrahedral geometry indicated that the energies of the near IR transitions supported a Cu site geometry which was close to tetrahedral. Second, since all the possible d–d transitions were observed at energies below 12 000 cm^{-1}, the dominant *visible* spectral features were attributed to charge-transfer transitions. Further, as other chemical and spectroscopic studies have indicated that cysteine (Cys) is a ligand to the blue copper, the visible absorption features at ~600 and ~800 nm ($\epsilon \sim 1000$ M^{-1} cm^{-1}) were interpreted as S(Cys) $\sigma \rightarrow$ Cu $d_{x^2-y^2}$ and $\pi \rightarrow$ Cu $d_{x^2-y^2}$ charge-transfer transitions, respectively. Third, the $g_{\parallel} > g_{\perp} > 2$ nature of the EPR spectrum indicated a nondegenerate $d_{x^2-y^2}$ ground state for the blue copper site. Finally, this ground state, combined with the axial nature of the EPR spectrum and the small $A_{\parallel}$ values, seemed to indicate[5,7] that the site was distorted from a pure tetrahedral geometry to one with an effective symmetry of D_{2d}.

Recently, the results of an X-ray crystal-structure determination have been reported for the blue copper protein, plastocyanin, from *Populus nigra*.[8] Following refinement of the structure at 1.6 Å resolution, the coordination of the copper atom in this protein is known, with estimated standard deviations of 0.02 Å in the positions of the coordinating atoms.[9] The distorted tetrahedral geometry of the copper site is confirmed, the ligand–Cu–ligand angles ranging from 85 to 132°. The Cu atom is coordinated by the side chains of the cysteine (Cys 84, Cu–S = 2.13 Å) and two histidines (His 37 and His 87, Cu–N = 2.04 and 2.10 Å), as well as methionine (Met 92, Cu–S = 2.90 Å). Combining these recent crystallographic results with new spectroscopic measurements and ligand field calculations, we have been able to correlate, in some detail, the electronic and geometric structures of the blue copper site.

We report here the results of polarized single-crystal optical and single-crystal EPR spectral studies and ligand field calculations on the blue copper site in poplar plastocyanin. First, a more detailed interpretation of the charge-transfer spectrum and an estimate of the relative contributions of the different types of ligands to the spectra and bonding are developed. The approximate orientation of the unique axis of the g tensor with respect to the blue copper site is then obtained, allowing the position of the $d_{x^2-y^2}$ orbital to be estimated; this orbital contains the unpaired

* Address correspondence to this author at the Massachusetts Institute of Technology.

(1) Malkin, R.; Malmström, B. G. *Adv. Enzymol.* **1970**, *33*, 177-244.
(2) Fee, J. A. *Struct. Bonding (Berlin)* **1975**, *23*, 1-60.
(3) Gray, H. B.; Solomon, E. I. In "Copper Proteins"; Spiro, T. G., Ed.; Wiley-Interscience: New York, in press.
(4) Solomon, E. I.; Hare, J. W.; Gray, H. B. *Proc. Natl. Acad. Sci. U.S.A.* **1976**, *73*, 1389-1393.
(5) Solomon, E. I.; Hare, J. W.; Dooley, D. M.; Dawson, J. H.; Stephens, P. J.; Gray, H. B. *J. Am. Chem. Soc.* **1980**, *102*, 168-178.
(6) Osborne, G. H.; Cheng, J. C.; Stephens, P. J. *Rev. Sci. Instrum.* **1973**, *44*, 10-15.
(7) Roberts, J. E.; Brown, T. G.; Hoffman, B. M.; Peisach, J. *J. Am. Chem. Soc.* **1980**, *102*, 825-829.
(8) Colman, P. J.; Freeman, H. C.; Guss, J. M.; Murata, M.; Norris, V. A.; Ramshaw, J. A. M.; Venkatappa, M. P. *Nature (London)* **1978**, *272*, 319-324.
(9) Guss, J. M.; Freeman, H. C., unpublished work.

0002-7863/81/1503-4382$01.25/0

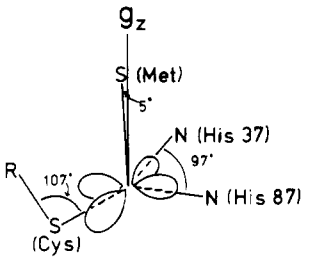

Figure 1. Electronic structural representation of the plastocyanin active site. The direction of g_z was determined experimentally, while the orientation of the $d_{x^2-y^2}$ orbital in the perpendicular plane was estimated from ligand field calculations as described in the text. Note that the bonds from Cu to N(His 37), N(His 87), and S(Cys) are all less than 15° below the xy plane.

electron and is involved in electron transfer. Next, a ligand field calculation, initially utilizing structurally defined model complexes, is used to determine an approximate energy level diagram for the blue copper site and correlate the effective symmetry with the real site symmetry. These studies lead us to represent the electronic structure of the plastocyanin copper site as in Figure 1. Finally, these studies also allow us to suggest what structural changes might produce the observed spectral differences among blue copper sites in different proteins.

II. Experimental Section

Poplar plastocyanin (*Populus nigra* var *italica*) was purified and crystallized from 2.6 M ammonium sulfate at pH 6.0 as described previously.[10]

The plastocyanin crystals used (orthorhombic space group $P2_12_12_1$; four molecules per unit cell) had either needle-like habits with their long axes parallel to the crystalline $\vec{a}$ axis and four well formed faces, (0,1,1), (0,1,$\bar{1}$), (0,$\bar{1}$,1) and (0,$\bar{1}$,$\bar{1}$), or were more nearly cubic in shape. Examination with a Vickers M72c polarizing microscope revealed that the crystals have a darker blue color when the incident light is polarized parallel to the $\vec{a}$ axis than when it is polarized perpendicular to $\vec{a}$.

Polarized optical spectra were recorded with a McPherson RS-10 spectrometer which had been modified[11] for use with small single crystals. The crystals examined were mounted in a pool of mother liquor between two quartz disks, which were separated by a lightly greased rubber gasket, with either the (0,1,1) or the (0,1,$\bar{1}$) face parallel to the flat surfaces of the disks. They were then masked off and mounted in a sample holder. Extinction directions were determined with a polarizing microscope and correlated with the crystallographic directions through the crystal morphology. Spectra were obtained with the incident light polarized parallel and perpendicular to the $\vec{a}$ axis (the symmetry defined dielectric directions) (Figure 2). In order to reduce the absorbances of all the bands to less than 2, and thus to permit them to be observed without distortion, some of the crystals were completely reduced by soaking in a buffered L-ascorbic acid solution [producing optically transparent crystals with d^{10} Cu(I) sites] and then reoxidized on their surfaces by a brief soaking in a buffered potassium ferricyanide solution. These crystals were studied over a period of weeks as they slowly became reoxidized while sealed between two quartz plates. This technique altered only the intensities, and not the shapes or positions, of the bands in the optical spectra. Polarized spectra were obtained from a crystal of irregular shape (approximately 1 × 0.6 × 0.1 mm) and several smaller, well formed crystals. The polarization ratios from the spectra of the smaller crystals were similar to those from the spectra of the large crystal.

EPR studies were carried out at approximately 9.2 GHz and 77 K on a Varian E-9 spectrometer. They were calibrated by recording a diphenylpicrylhydrazide (DPPH) signal (g = 2.0037) at the beginning and end of each session. Initially, the crystals were mounted on thin quartz plates which were attached by means of a small amount of grease to a second quartz plate joined to a long quartz rod. This assembly was inserted into an EPR tube which was then oriented within a liquid N_2 Dewar. The orientation of the $\vec{a}$ axis was determined through the use of a polarizing microscope; in studies in which the $\vec{a}$ axis was parallel to the axis of rotation of the sample, the $\vec{b}$ and $\vec{c}$ axes were found by determining the positions about which rotations of a given angle both clockwise and counterclockwise yielded identical spectra. In later studies, the crystals were mounted in quartz capillary tubes sealed with stopcock grease, and the orientations of the crystals axes were determined by X-ray diffraction. All other experimental techniques were as described above. However, this technique yielded spectra with broader signals. EPR spectra of each crystal were taken at 10° intervals with respect to rotation about an axis normal to the magnetic field. Crystals were mounted in the following orientations: $\vec{a}$ axis parallel to the axis of rotation, $\vec{b}$ axis parallel to the axis of rotation, $\vec{a}$ axis perpendicular to and $\vec{b}$ axis 15° off the axis of rotation, and $\vec{a}$ axis about 54° and $\vec{b}$ axis 35° off the axis of rotation. Spectra from all of these rotations were simulated by using the SIM14A computer program (obtained from the Quantum Chemistry Program Exchange) after it had been modified to simulate single-crystal spectra.

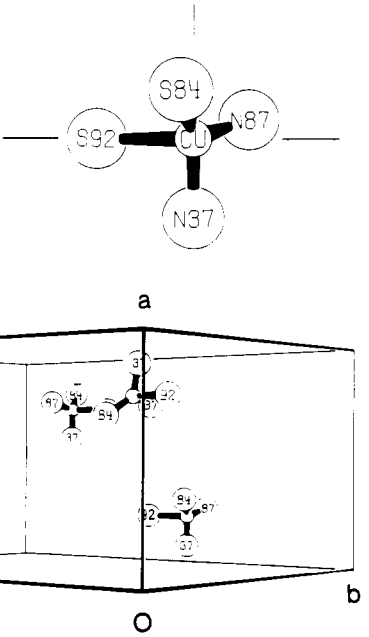

Figure 2. Plastocyanin unit cell projected on (011) plane, showing positions of four symmetry-related Cu atoms and their first coordination shells. The Cu-ligand bonds are drawn on twice the scale of the unit cell (lower). Expanded view of Cu atom and ligands at x, y, z in relation to the axial directions: x axis horizontal, y and z axis in directions away from observer (upper).

III. Results and Discussion

A. Polarized Single-Crystal Electronic Spectroscopy. Knowledge of the dependence of the visible absorption spectrum on the orientation of polarized light with respect to the crystallographically defined blue copper sites in plastocyanin enables us to relate much of this spectrum to specific ligands. An interpretation of these unique spectral features, on the basis of specific types of charge-transfer transitions for each ligand, can then be presented as all of the ligand field (d–d) transitions have been associated with spectral features at lower energies (12 000 cm^{-1} and below, see section IIIC).[4,5]

The polarized single-crystal spectrum of plastocyanin has four distinct regions (27–24 000, 24–20 000, 20–15 000, and 15–12 000 cm^{-1}, Figure 3A). Simultaneous Gaussian analysis of the low temperature film absorption, CD, and MCD spectra of plastocyanin[5] have shown that each of the two lowest energy regions can be decomposed into two absorption bands (Figure 3B). Clearly, band 1 (using the numbering scheme indicated in Figure 3) is polarized strongly perpendicular to the $\vec{a}$ axis, band 2 is strongly parallel, and bands 3–5 have mixed, slightly parallel polarizations. The polarization ratios [$I_{\parallel}/I_{\perp}$ where $I_{\parallel(\perp)}$ indicates absorption band intensity in the parallel (perpendicular) polarization] for each transition were estimated by resolving the parallel and perpendicular scans of two sets of spectra into the Gaussians obtained from the simultaneous analyses of the absorption, CD, and MCD spectra. Values of these ratios are given in Table I. Note that there is more error in the estimate of $I_{\parallel}/I_{\perp}$ for band 3 than in those for the other bands, as band 3 is obscured by its overlap with the more intense band 4.

(10) Chapman, G. V.; Colman, P. M.; Freeman, H. C.; Guss, J. M.; Murata, M.; Norris, V. A.; Ramshaw, J. A. M.; Venkatappa, M. P. *J. Mol. Biol.* **1977**, *110*, 187-189.

(11) Wilson, R. B.; Solomon, E. I. *Inorg. Chem.* **1978**, *17*, 1729-1737.

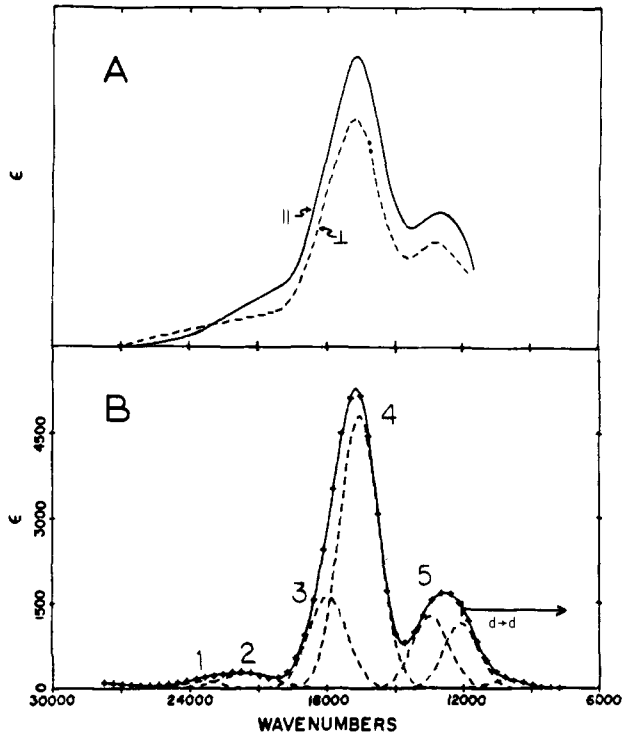

Figure 3. (A) Optical spectrum of a single crystal of plastocyanin obtained with light incident to the (0,1,1) face and polarized parallel (solid line) and perpendicular (dashed line) to $\vec{a}$. (B) Gaussian resolution of the 35-K visible absorption spectrum of a plastocyanin film; the symbols (+) represents the experimental absorption spectrum.

Table I. Polarization Ratios

band no.	$\bar{\nu}$, cm^{-1}	obsd $I_{\parallel}/I_{\perp}$[a]
1	23 340	0.0-0.4
2	21 390	1.6-2.3
3	17 870	1.1-1.8
4	16 490	1.27-1.32
5	13 350	1.2-1.6

ligand	calcd $I_{\parallel}/I_{\perp}$
Met(92)	0.00
His(37)	84.83
His(87)	0.12
His(37) + His(87)	2.49
Cys(84)	0.96

[a] Ranges of values were determined from Gaussian analyses of the two sets of spectra.

Calculations of polarization ratios for the charge-transfer transitions from the four ligands require consideration of the symmetry of the unit cell. The four molecules in the $P2_12_12_1$ unit cell are related by three screw axes parallel to the three orthogonal crystal axes. The two molecules related to each other by the screw axis parallel to $\vec{a}$ are spectroscopically equivalent with respect to light polarized either parallel or perpendicular to $\vec{a}$ and normal to either the (0,1,1) or (0,1,$\bar{1}$) face. They are not optically equilvalent to the other two molecules in the unit cell. Thus there are two sets of two optically equivalent molecules. In addition, each of the molecules in either of these sets is related to each of the molecules in the other set by a screw rotation parallel to either $\vec{b}$ or $\vec{c}$. Since the $\vec{b}$ and $\vec{c}$ axes bisect the angles between adjacent faces, the orientation, with respect to a given face, of a molecule in one set is optically equivalent to the orientation with respect to an adjacent face of either molecule in the other set. The same spectrum is therefore produced, no matter whether the light is propagated into the (0,1,1) face or the (0,1,$\bar{1}$) face. In Figure 2, the copper sites of four symmetry-related molecules are projected on the (0,1,1) face.

When calculating the polarization ratios we assume that the transition dipole moments are directed along the metal–ligand

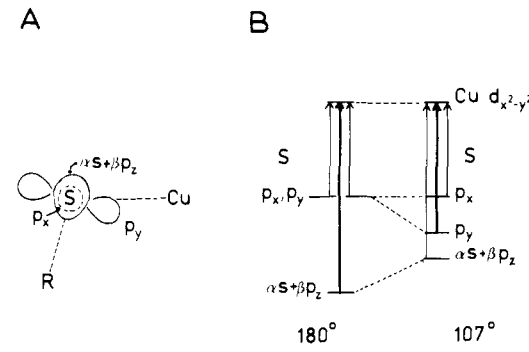

Figure 4. (A) Binding of cysteine sulfur to the copper. Three sulfur orbitals are involved, where R designates the rest of the cysteine residue and the R–S–Cu bond angle is 107°. (B) Relative energies of the sulfur orbitals involved in ligand-to-metal charge-transfer transitions. R–S–Cu bond angle of 180° (left); R–S–Cu bond angle of 107° (right).

axes. This should be a reasonable approximation which, however, ignores the effects of deviation from axial symmetry along each metal–ligand bond and the interactions among charge-transfer transitions from different ligands. The polarization intensity ratio ($I_{\parallel}/I_{\perp}$) to be expected for a charge-transfer transition from a specific ligand is then given by

$$I_{\parallel}/I_{\perp} = 2t^2/(S_A^2 + S_B^2)$$

where t is the projection of the copper ligand bond onto the $\vec{a}$ axis (all sites equivalent), and $S_{A(B)}$ is the projection perpendicular to $\vec{a}$ on the (0,1,1) face for site A (B). The predicted ratios for the four ligands of the blue copper atom are included in Table I. The calculated polarization ratio for two histidines contributing equally to the same transition is also given.

Our polarized single-crystal optical spectral results for plastocyanin clarify the assignments of bands 3, 4, and 5 (Figure 3 B) and limit the possible assignments for the weaker bands 1 and 2. First, the mixed polarizations of bands 4 and 5, combined with their low energies, confirm their assignments as cysteine S → Cu charge-transfer transitions. Next, it is apparent from the lack of significant perpendicular polarization in the region of bands 3–4 that the methionine does not contribute measurably to this region. While it was originally[5] suggested on the basis of model studies that band 3 might originate from a methionine S → Cu charge-transfer process, the long Cu–Met bond and the poor orientation of the $d_{x^2-y^2}$ orbital (vide infra) with respect to this bond appear to preclude this possibility. Thus, while the intensity of this band may have been overestimated in the Gaussian resolved absorption spectra of this study and ref 5, its presence in these spectra and in the circular dichroism spectra of all blue copper sites (including stellacyanin, which contains no methionine), indicates that it must be related to either cysteine S → Cu or histidine N → Cu charge-transfer transitions. The observed polarization ratio of band 3 is consistent with either possibility, provided that both histidines would contribute about equally to this absorption or borrow intensity from cysteine S → Cu charge transfer (band 4). absorption or borrow intensity from cysteine S → Cu charge transfer (band 4). However, model studies indicate that the intensity of band 3 is too high and the energy too low for a histidine N → Cu charge-transfer assignment.[12] Thus, the polarized single-crystal data support the assignments of bands 3, 4, and 5 as cysteine S → Cu charge-transfer transitions. Only two bands of this type were predicted by the simple σ,π model used in previous treatments,[4,5] permitting speculation concerning the assignment of band 3. However, the original σ,π model (left-hand side of Figure 4B) assumed a C–S–Cu bond angle of 180° at the sulfur atom of the cysteine residue. The crystal structure analysis has shown that this bond angle is, in fact, 107°.[9] The occupied sulfur orbital set of highest energy (p_x, p_y) should,

(12) Fawcett, T. G.; Bernarducci, E. E.; Krogh-Jespersen, K.; Schugar, H. J. *J. Am. Chem. Soc.* **1980**, *102*, 2598-2604.

therefore, be split, p_y being significantly stabilized because of its σ *overlap* with the copper orbitals (right-hand side of Figure 4 B). Excitation from this $S(p_y)$ to $Cu(d_{x^2-y^2})$ gives rise to the most intense absorption, band 4, because the largest overlap is involved. The excitation of an electron from the p_x orbital produces a weak π-type transition at lower energy, consistent with the magnetic dipole character of band 5.[4] The bonding of the sulfur atom to the carbon on the cysteine residue causes the s and p_z orbitals on the sulfur atom to mix,[13] placing the third pair of electrons on the sulfur into an $\alpha s + \beta p_z$ hybird orbital at a higher binding energy. The transition from this orbital should then appear at the highest energy of the three observed charge-transfer transitions originating from the sulfur atom and should be less intense than the $S(p_y) \rightarrow Cu$ charge-transfer transition due to its more limited overlap with $Cu(d_{x^2-y^2})$. This cysteine $S(\alpha s + \beta p_z) \rightarrow Cu(d_{x^2-y^2})$ charge-transfer transition is a possible assignment for band 3. While detailed single-crystal electronic spectral studies on a thiolate–copper complex are required to obtain an experimental estimate for the energy of such a cysteine $S(\alpha s + \beta p_z) \rightarrow Cu(d_{x^2-y^2})$ charge-transfer transition, three cysteine $\rightarrow$ Cu transitions seem to be observed in a 5000-cm^{-1} region of the spectrum of a model complex (Figure 3 of ref 14). We are presently attempting to characterize these transitions through both optical absorption experiments and self-consistent-field $X\alpha$ Scattered Wave calculations.

Bands 1 and 2 must be derived from some combination of charge-transfer processes involving the remaining three ligands, His(37), His(87), and Met(92). The observed polarization ratios are most consistent with the assignments of band 1 to S(Met) $\rightarrow$ Cu charge transfer and band 2 to N(His) $\rightarrow$ Cu charge transfer, with the latter transition resulting from approximately equal transition probability contributions from both histidines. This assignment places the methionine charge-transfer transition at a higher energy than has been suggested from most model studies.[15-17] Two charge-transfer transitions are possible from a thioether ligand: a low energy $p_z \rightarrow Cu(d_{x^2-y^2})$ and a higher energy $\alpha s + \beta p_{x,y} \rightarrow Cu(d_{x^2-y^2})$. In model complexes, thioether sulfur atoms are bonded to copper with a geometry which should favor greater intensity in the lower energy $p_z \rightarrow$ Cu charge-transfer transition.[16-19] A change in the nature of this transition, resulting in a blue shift, may be induced by the longer Cu–S bond and the greater angle between the sulfur p_z orbital and the Cu–S direction in plastocyanin.[9] An alternative possibility is that bands 1 and 2 are both associated with the histidines. Low-energy charge-transfer transitions from both the imidazole π_1 and π_2 molecular orbitals are possible, with the $\pi_2 \rightarrow Cu\ d_{x^2-y^2}$ transition occuring at higher energy.[12] The two transitions should be split by >4000 cm^{-1} and should have the same polarization ratios and similar intensities. This suggests either that (i) the His(87) $\pi_1 \rightarrow Cu\ d_{x^2-y^2}$ transition is associated with band 1 (strong in perpendicular polarization) and the His(37) $\pi_1 \rightarrow Cu\ d_{x^2-y^2}$ transition accounts for band 2 (strong in parallel polarization) with the corresponding transitions from the π_2 orbitals contributing to the weak absorption in the >28 000 cm^{-1} region, or (ii) that bands 1 and 2 are due to the transitions His(87) $\pi_2 \rightarrow Cu\ (d_{x^2-y^2})$ and His(37) $\pi_2 \rightarrow Cu\ (d_{x^2-y^2})$ respectively, with the transitions from the π_1 levels (rather than the highest energy cysteine charge transfer) contributing to band 3. For the first of these two assignments the observed energies are more consistent with the results of model studies.[12]

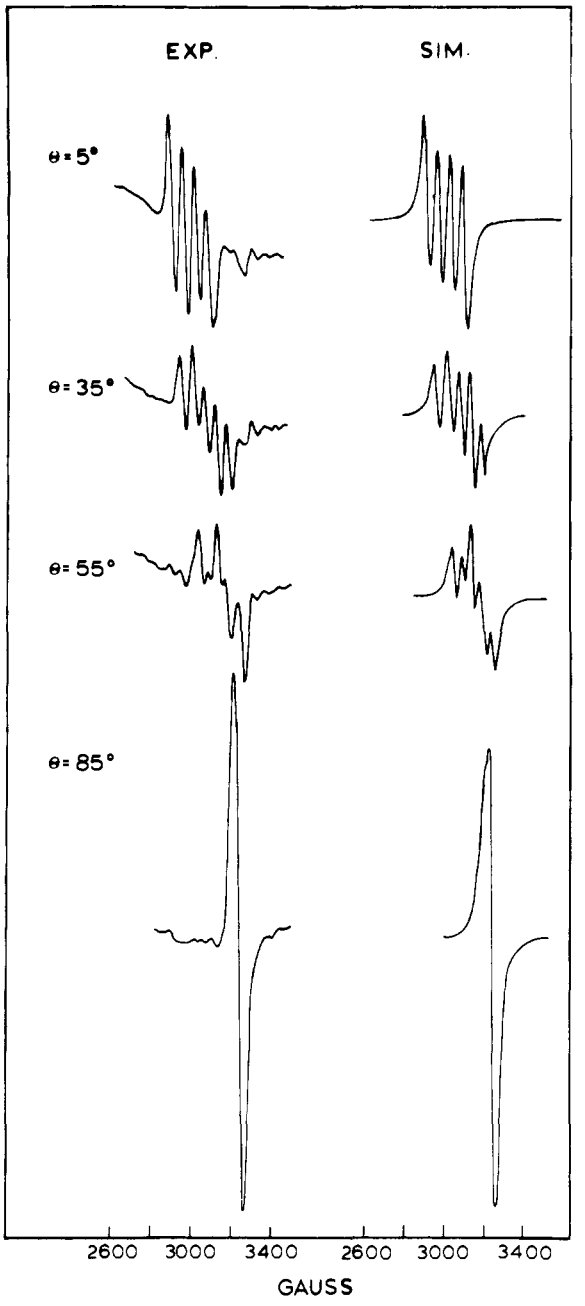

Figure 5. Representative experimental and simulated EPR spectra of a single crystal of plastocyanin. Crystal $\vec{a}$ axis is parallel to the axis of rotation and normal to the magnetic field and θ equals the angle between the magnetic field vector and the crystal $\vec{c}$ axis. Simulation performed with four molecules in a unit cell, g_z 8° off $\vec{c}$ in the *bc* plane and 5° out of the *bc* plane, and *g* and *A* tensors collinear.

In either case the quantitative agreement of band 2 with the calculated polarization ratio is poor, however, ($I_\parallel/I_\perp$, predicted = 84.8; observed = 2.3). Detailed spectroscopic studies on crystallographically defined model complexes are required to comment further on these assignments.

B. Single-Crystal EPR Spectroscopy. Single-crystal EPR experiments were performed to determine the orientation of the *g* tensor with respect to the plastocyanin copper site and the approximate orientation of the *A* tensor relative to this *g* tensor. Since the four molecules in the unit cell have different, but symmetry related, orientations, the orientations of the g_z vectors of the molecules must be symmetry related—but not necessarily identical—with respect to the external magnetic field. As indicated in Figure 2, only when the magnetic field is directed along a crystal axis are all of the molecules required by symmetry to be magnetically equivalent. When the magnetic field is parallel to the

(13) Bair, R. A.; Goddard, W. A., III *J. Am. Chem. Soc.* **1978**, *100*, 5669-5676.
(14) Hughey, J. L. IV; Fawcett, T. G.; Rudich, S. M.; Lalancette, R. A.; Potenza, J. A.; Schugar, H. J. *J. Am. Chem. Soc.* **1979**, *101*, 2617-2623.
(15) Amundsen, A. R.; Whelan, J.; Bosnich, B. *J. Am. Chem. Soc.* **1977**, *99*, 6730-6739.
(16) Miskowski, V. M.; Thich, J. A.; Solomon, R.; Schugar, H. J. *J. Am. Chem. Soc.* **1976**, *98*, 8344-8350.
(17) Ferris, N. S.; Woodruff, W. H.; Rorabacher, D. G.; Jones, T. E.; Ochrymowycz, L. A. *J. Am. Chem. Soc.* **1978**, *100*, 5939-5942.
(18) Glick, M. D.; Gavel, D. P.; Diadderio, L. L.; Rorabacher, D. B. *Inorg. Chem.* **1976**, *15*, 1190-1193.
(19) Ou, C. C.; Miskowski, V. M.; Lalancette, R. A.; Potenza, J. A.; Schugar, H. J. *Inorg. Chem.* **1976**, *15*, 3157-3161.

Table II. Ligand Field Parameters

	model			plastocyanin		
ligand	bond length, Å	α_2, cm^{-1}	α_4, cm^{-1}	bond length, Å[a]	α_2, cm^{-1}	α_4, cm^{-1}
His	2.01[b,c]	14 000	7500	1.97	14 915	8334
Cys	2.36[d]	12 000	6000	2.10	10 000	7500
Met	2.30[e] (2.37)[f]	13 400	6700	2.90	4 000	1000

[a] These bond lengths were determined through EXAFS studies. Calculations using parameters corresponding to the bond lengths determined through more recent X-ray crystallographic studies (Cys 84, Cu-S = 2.13 Å; His 37 and His 87, Cu-N = 2.04 and 2.10 Å) gave similar results and rotated g_z by less than 3°. [b] Ligand field fit to tetrakis(imidazole)dinitratocopper(II) model complex spectrum[25] included α_2(Cu-O) = 3500 and α_4(Cu-O) = 2400 cm^{-1} (Cu-O bond length = 2.6 Å) for axial nitrates. [c] Spectral fit for hexakis(imidazole)copper(II) nitrate[24] included α_2 = 13 250 and α_4 = 6850 cm^{-1} for Cu-N bond length of 2.05 Å and α_2 = 6550 and α_4 = 2110 cm^{-1} for Cu-N bond length of 2.59 Å. [d] Spectral fit of (*rac*-5,7,7,12,14,14-hexamethyl-1,4,8,11-tetraazocyclotetradecane)copper(II) *o*-mercaptobenzoate hydrate, [Cu(tet b)(*o*-$SC_6H_4CO_2$)]·H_2O[14] included α_2 = 13 350 and α_4 = 6520 cm^{-1} for Cu-N = 1.99 Å, α_2 = 12 700 and α_4 = 6020 cm^{-1} for Cu-N = 2.03 Å, α_2 = 10 940 and α_4 = 4670 cm^{-1} for Cu-N = 2.13 Å, and α_2 = 10 040 and α_4 = 4050 cm^{-1} for Cu-N = 2.19 Å. These values were determined from a spectral fit of $Na_4Cu(NH_3)_4[Cu(S_2O_3)_2]_2$·$H_2O$ and $Na_4Cu(NH_3)_4[Cu(S_2O_3)_2]_2$·$NH_3$.[26] [e] Spectral fit of (1,4,8,11-tetrathiacyclotetradecane)copper(II) diperchlorate[17,18] included α_2 = 3180 and α_4 = 2040 cm^{-1} for Cu-O = 2.65 Å. [f] Spectral fit of bis[β-(methylmercapto)ethylamine]copper(II) diperchlorate[16,19] included α_2 = 13 710 and α_4 = 6820 cm^{-1} for Cu-N = 1.98 Å and α_2 = 3370 and α_4 = 2250 cm^{-1} for Cu-O = 2.60 Å.

plane containing two crystal axes but not directed along either axis, the molecules in the unit cell divide into two nonequivalent sets of two magnetically equivalent sites. This produces a spectrum which is the sum of the spectra produced by the two sets. For more general directions of the magnetic field, the four sites in the unit cell will all be magnetically nonequivalent.

The left column of Figure 5 shows the spectra obtained with the crystal $\vec{a}$ axis perpendicular to the magnetic field and the $\vec{b}$ and $\vec{c}$ axes at various angles with respect to the magnetic field vector, $\vec{H}$. Clearly the spectrum with $\vec{H}$ nearly parallel to $\vec{c}$ is close to a pure $g_\parallel$ spectrum while that with $\vec{H}$ 5° off $\vec{b}$ shows almost a pure $g_\perp$ signal. The right column of this figure shows simulations of experimental spectra with the projection of g_z on the *bc* plane being 8° off $\vec{c}$ and with g_z 5° out of the *bc* plane and A_z parallel to g_z. Spectra were also obtained and stimulated with crystals in the other orientations described in the Experimental section. All of the results are consistent with g_z being located 8° (±2°) away from $\vec{c}$ in the *bc* plane and 5° (±3°) out of the *bc* plane and with the *A* tensor oriented approximately along the *g* tensor. No evidence for rhombic splitting of the *g* tensor was observed.

Owing to the symmetry of the unit cell, EPR experiments alone cannot do more than limit the possible positions of the g_z vector to four orientations with respect to a given molecule. However, crystal field calculations of the blue copper site (see next section) support the orientation with g_z directed about 5° away from the Cu–S(Met 92) bond, 91° from the Cu–N(His37) bond, and 102° from the Cu–N(His87) bond (see Figure 1). Significantly, this orientation of g_z provides a fairly clear interpretation of the linear electric field effects observed for the blue copper protein sites in frozen solution.[20] In these experiments the largest shift is observed with the electric field perturbation perpendicular to g_z. Thus, the dominant contribution to this shift cannot be associated with $4p_z$ mixing (p_z is oriented along g_z), but probably is due to a S(Cys 84) → Cu component in the ground-state wave function, as the S(Cys 84)–Cu bond is aligned ~104° away from g_z.

C. Blue Copper Ligand Field Having the combination of fairly accurate spectral assignments and a crystallographically defined copper site geometry, we can now generate a picture of the electronic structure of the blue copper site by means of a ligand field theoretical treatment. This treatment provides an estimate of the contribution of each ligand to the blue copper ligand field, identifies the correct orientation of the g_z axis and therefore the orientation of the d orbital involved in redox processes, provides further insight into the nature of the near IR d–d transitions, and establishes a reasonable description of the effective symmetry of this active site.

The energy levels and wave functions were calculated by using the method of Companion and Komarynsky.[21] In this strong field method, no simplifying assumptions about site symmetry are made, and each element of the secular determinant, $|H_{pq} - S_{pq}E_k|$, is calculated, using the real d orbitals as the basis set. Each ligand *i* is treated as a point charge, and its electrostatic interaction with the metal d electrons is viewed as a perturbation on the d energy levels. After expanding each of the potentials, $V_i = Z_i e^2/r_{ij}$ (where r_{ij} is the distance between the ligand *i* and each of the electrons, *j*, in the metal d orbitals) in terms of spherical harmonics, and summing them, the following expression for the general matrix element, H_{pq}, is obtained:

$$\langle\psi_p|H|\psi_q\rangle = \sum_{i=1}^{N}\sum_{l=0,2,4}\sum_{m=-l}^{l}\frac{4\pi Z_i e^2}{2l+1}Y_{lm}^*(\theta_i,\phi_i)\int\psi_p^*[r_<^l/r_>^{l+1}]_i Y_{lm}(\sigma,\phi)\psi_q d\upsilon$$

where N = the total number of ligands. The radial and angular parts of this integral can be separated and a quantity α_l^i defined such that

$$\alpha_l^i = Z_i e^2\int_0^\infty R_{3d}^2[r_<^l/r_>^{l+1}]_i r^2 dr$$

Given the spatial coordinates and values of α_0, α_2, and α_4 for each ligand, each of the elements of the secular determinant can be readily calculated (see Tables 1 and 2 of Companion and Komarynsky[22]). Diagonalization of the resulting Hamiltonian matrix yields the linear combinations of the real d orbitals which correspond to each of the five energy levels. Rotation of the coordinate system changes these linear combinations but not the energy of each level. The values of the matrix elements of the g tensor were calculated by using the perturbative approach outlined by Ballhausen.[23] For the general matrix element g_{ij} (where $i,j = x,y,z$), we have

$$g_{ij} = 2\left(\delta_{ij} - \lambda\sum_{n\neq 0}\frac{\langle\psi_0|L_i|\psi_n\rangle\langle\psi_n|L_j|\psi_0\rangle}{E_n - E_0}\right)$$

where the summation is over the excited d–d states. Once the *g* tensor was calculated and diagonalized, the coordinate system for quantization of the real d orbitals was rotated into alignment with the principal directions of this tensor.

Since the parameters α_0^i contribute equally to each of the diagonal elements of the Hamiltonian matrix, they do not affect the splittings between the d orbitals and are set equal to zero. The initial values for α_2^i and α_4^i were determined through the use of model complexes for the three ligand types (imidazole, thioether, and thiolate; total = 6 parameters).[14-18,24-27] The complexes used

(20) Peisach, J.; Mims, W. B. *Eur. J. Biochem.* **1978**, *84*, 207-214.
(21) Companion, A. L.; Komarynsky, M. A. *J. Chem. Educ.* **1964**, *41*, 257-262.
(22) Note error in the expression for G_{21}^i in Table I of ref 21. This should be $G_{21}^i = \alpha_2^i \sin\theta_i \cos\theta_i \sin\phi_i$.
(23) Ballhausen, C. J. In "Introduction to Ligand Field Theory" McGraw-Hill: New York, 1962.
(24) McFadden, D. L.; McPhail, A. T.; Garner, C. D.; Mabbs, F. E. *J. Chem. Soc., Dalton Trans.* **1975**, 263-268.
(25) McFadden, D. L.; McPhail, A. T.; Garner, C. D.; Mabbs, F. E. *J. Chem. Soc., Dalton Trans.* **1976**, 47-52.
(26) Hathaway, B. J.; Stephens, F. *J. Chem. Soc. A* **1970**, 884-888.

Table III. Effects of Variation of Ligand Field Strength of Substituted Ligand on the Blue Copper Spectral Properties

spectral property	exptl values		calcd values[a]		
			ligand field parameters at methionine position		
	plastocyanin	stellacyanin	$\alpha_2 = 4000\ cm^{-1}$[b] $\alpha_4 = 1000\ cm^{-1}$	$\alpha_2 = 6500\ cm^{-1}$ $\alpha_4 = 2110\ cm^{-1}$	$\alpha_2 = 12310\ cm^{-1}$ $\alpha_4 = 6060\ cm^{-1}$
d-d transition energies, cm^{-1}	5000[c]	5250[c]	3500	3500	2600
	9150	8100	9100	7700	5000
	11200	10500	10000	9400	8400
			11400	10700	9700
g_x	2.053[d]	2.025[e]	2.028[f,g]	2.029	2.028
g_y	2.053	2.077	2.053	2.061	2.103
g_z	2.226	2.287	2.226	2.225	2.222

[a] In these calculations, the ligand positions of the plastocyanin site were used; the histidine and cysteine ligand field parameters used were those given for the plastocyanin site in Table II while those for the ligand at the methionine position were varied as indicated. [b] These values of the parameters were used in the calculation of the plastocyanin site. [c] From ref 5. [d] From ref 2. [e] From Malmstrom, B.; Reinhammar, B.; Vänngård, T. *Biochim. Biophys. Acta* 1970, *204*, 48-57. [f] Calculated by using Stevens' orbital reduction factors of $k_{\parallel}^2 = 0.136$ and $k_{\perp}^2 = 0.241$. [g] A small rhombic splitting ($g_x - g_y = 0.017$) has been reported for *Pseudomonas aeruginosa* azurin (Brill, A. S. "Transition Metals in Biochemistry"; Springer-Verlag: New York, 1977; p 49).

as models all had X-ray crystallographically determined structures. The values of α_2 and α_4 were systematically varied for each model complex until the set which produced the best match between the calculated energy level splitting and the ligand field optical spectrum was determined (see Table II). Only in the case of the thiolate ligand is there significant flexibility in the resulting ligand field parameters. In the tet-b model complex, the thiolate sulfur is one of five ligands bonded to the copper.[14] The effects of error in the ligand field parameters of the thiolate sulfur ligand may be hidden by compensatory changes in the parameters of the other four ligands.

The ligand field parameters calculated for the models are appropriate only for the metal–ligand distances found in these complexes. The values of the parameters appropriate for the bond lengths found in the blue copper site were initially estimated by extrapolation, using the crude approximations that α_2 and α_4 are proportional to $1/R^3$ and $1/R^5$, respectively, where R is the bond length. The extrapolated values of α_2 and α_4 for the histidines should be quite accurate, since the values in the model complexes are well defined and the differences between the bond lengths in the plastocyanin site and those in the model systems were very small. For cysteine and methionine, the extrapolated values of α_2 and α_4 were allowed to vary until the best fit to the near-IR d–d transitions, the g tensor orientation, and the g values was obtained. The cysteine parameters were then extrapolated back to values appropriate for the copper–sulfur bond length of the tet-b model complex,[14] and a reasonable overall fit for the thiolate ligand field was obtained. The final plastocyanin and model ligand field parameters are given in Table II.

Our results indicate that the histidines make the largest contribution to the blue copper ligand field, the cysteine is strong but somewhat weaker than histidine despite its short 2.1-Å bond length, and the methionine, at 2.9 Å from the copper, makes a small but real contribution to the ligand field. The g tensor calculated with these ligand field parameters can be diagonalized with g_z oriented approximately 16° off the Cu–S(Met 92) bond. This is close to the experimentally determined orientation described in section IIIB. The calculated g values are $g_x = 2.053$, $g_y = 2.028$, and $g_z = 2.226$ by using Stevens' orbital reduction factors of $k_{\parallel}^2 = 0.136$ and $k_{\perp}^2 = 0.241$ (plastocyanin (experimental): $g_{\parallel} = 2.226$, $g_{\perp} = 2.053$).[2]

The calculated energy level diagram for the ligand field ground and excited states is given in the center of Figure 6, where the squares of the coefficients of the dominant d orbital contributions to each wave function are given, using the coordinate system which diagonalized the g tensor. Clearly, the EPR parameters given above result from the nondegenerate, almost pure $d_{x^2-y^2}$ nature of the ground state. The orientation of the $d_{x^2-y^2}$ orbital with respect to the geometric structure is indicated in Figure 1 and

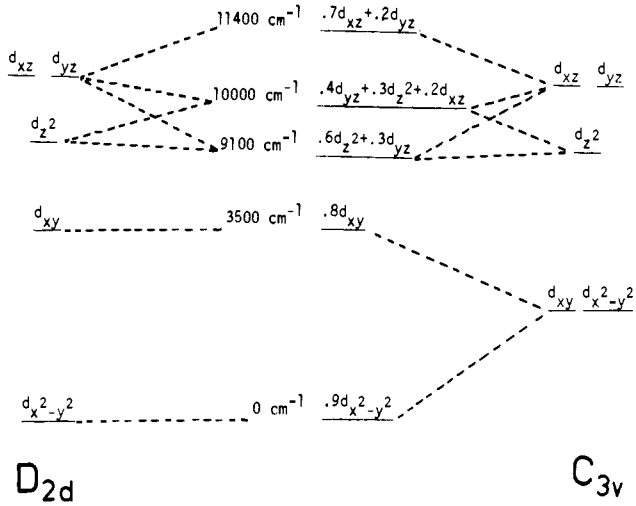

Figure 6. Ligand field energy level diagram calculated for plastocyanin. Center contains energies and wave functions (squared coefficients of leading terms) of plastocyanin site. Energy levels determined after removing the rhombic distortions to give D_{2d} and C_{3v} symmetries are shown in left and right columns, respectively.

may provide insight into possible electron-transfer pathways.

The excited states shown in Figure 6 correspond to the near IR CD spectral features observed[4,5] for plastocyanin at 5000, 9000, and 11 200 cm^{-1}. At this point the association of specific energy levels with specific spectral features is not clear. However, it appears that the lowest energy transition is $d_{x^2-y^2} \rightarrow d_{xy}$ and probably corresponds to the 5000-cm^{-1} CD feature and the higher energy 9–12 000-cm^{-1} transitions are quite mixed. As a theoretical estimate of this mixing is strongly dependent on specific values of the ligand field parameters and an even more precise knowledge of the geometry than is now available, this mixing is best determined experimentally through further near IR MCD studies.

We can now consider how this rhombically distorted site is related to an effective site of higher symmetry. There are two distortions from a tetrahedral geometry which produce sites with axial symmetry, the point groups of the resultant sites being D_{2d} and C_{3v}. We start by assuming that the blue copper energy level diagram is associated with a rhombically perturbed version of one of these limiting geometries and then remove the effects of these perturbations. The resultant energy level diagrams for the D_{2d} and C_{3v} limits are included in Figure 6. The D_{2d} limit cannot be correct as a D_{2d} distorted tetrahedron should have a state diagram with $d_{x^2-y^2} < d_{xz,yz} < d_{z^2} < d_{xy}$.[5] The diagram for the C_{3v} limit, however, does correspond to that of a tetrahedron with an elongated bond (C_{3v} distortion) and the metal lowered toward the plane of the remaining three ligands. Thus "elongated C_{3v} with significant rhombic distortions" is the most appropriate description

(27) Smith, D. W. *J. Chem. Soc., Dalton Trans.* **1973**, 1853-1858.

of the plastocyanin active site. While the elongated bond in the C_{3v} distorted tetrahedron is obviously associated with the long copper–methionine bond, further ligand field calculations indicate that the rhombic distortions are associated with differences between the ligand field strengths as well as the geometry of the cysteine and two histidine ligands. As long as the cysteine has a weaker ligand field strength than the histidines, the rhombically distorted site produces an axial-type EPR spectrum with $g_{\parallel} > g_{\perp} > 2$. This pattern is the result of the large rhombic splitting of the ^2E $(xy, x^2 - y^2)$ C_{3v} ground-state degeneracy, which yields a $d_{x^2-y^2}$ ground state, and the small splitting of the ^2E (xz, yz) pair. Only energetic differences in the latter pair can cause the inequivalence of g_x and g_y.

Finally, while the mixing of p_z character into the $d_{x^2-y^2}$ ground state is generally considered to be necessary to decrease A values in tetrahedral copper complexes,[28-32] it should be noted that an elongated C_{3v} geometry alone is not sufficient to provide this mixing. The rhombic distortion does make this possible; however, a detailed molecular orbital calculation is required to obtain an accurate estimate of the copper ground-state wave function for this geometry and thus the relative contributions of excited state configurations to the reduction in hyperfine splitting.

D. Extensions to Blue Copper Sites in Other Proteins. The generation of a fairly detailed interpretation of the spectra of the blue copper site in plastocyanin in terms of specific structural features gives us further insight, on the basis of spectral changes, into possible structural variations among blue copper sites in other proteins.

The azurins have charge-transfer, ligand field, and EPR spectra which are extremely similar to those of plastocyanin.[4,5] This lends strong support to the latest X-ray crystallographic treatment of *Pseudomonas aeruginosa* azurin, which incorporates the plastocyanin copper site into the structure determination.[33] Both proteins also exhibit very similar reduction potentials (plastocyanin = 347 mV; azurin = 330 mV[34]). On the other hand, stellacyanin and the analogous basic blue protein, mavicyanin, and rusticyanin[35] differ from plastocyanin in having measurable rhombic EPR signals,[2] ligand field transitions at lower energy,[4,5] and one relatively intense absorption at ~450 nm in place of charge-transfer transitions 1 and 2.[4,5] Ligand field calculations show (see Table III) that the required substitution of the methionine (stellacyanin does not contain this amino acid[36]) with a stronger field ligand would shift the ligand field transitions to lower energy and produce a rhombic splitting of g_x and g_y. Changes in thiolate ligation between stellacyanin and plastocyanin are unlikely, however, as there is little change in the 600- and 800-nm spectral features associated with the S(Cys) → Cu charge-transfer transitions. In contrast, studies of fungal laccase show significant changes in this S(Cys) → Cu charge-transfer region, particularly in the CD spectrum.[38] These spectral differences could be related to either structural variation in a single S(Cys)–Cu bond or the presence of an additional sulfur ligand.

Finally, the generally high reduction potentials of the blue copper sites have been attributed to the low ligand field stabilization energies associated with the copper(II) in a tetrahedral geometry[5] with a thiolate ligand. The further differences between the potentials of the blue copper sites in stellacyanin (184 mV)[34,39] and fungal laccase (785 mV)[39] and those of the sites in the plastocyanins and azurins seem to be at least partially correlated to the variations in blue copper ligation as discussed above.

Acknowledgment. E.I.S. thanks Harry B. Gray and Harvey J. Schugar and Harvey J. Schugar for valuable discussions on blue copper spectra during the course of this study and the National Science Foundation (PCM 7813714) for support of this research. H.C.F. acknowledges helpful assistance from Dr. J. M. Guss and Dr. M. Murata and support from the Australian Research Grants Committee (Grant 74/15398). We also thank Professor G. Petsko and T. Alber for X-ray determination of crystal orientations at MIT.

(28) Bates, C. A.; Moore, W. S.; Standley, K. J.; Stevens, K. W. H. *Proc. Phys. Soc.* **1962**, *79*, 73-83.
(29) Bates, C. A. *Proc. Phys. Soc.* **1964**, *83*, 465-472.
(30) Sharnoff, M. *J. Chem. Phys.* **1965**, *42*, 3383-3395.
(31) Parker, J. H. *J. Phys. C* **1971**, *4*, 2967-2978.
(32) Krishnan, V. G. *J. Chem. Phys.* **1978**, *68*, 660-662.
(33) Adman, E. T.; Stenkamp, R. E.; Sieker, L. C.; Jensen, L. H. *J. Mol. Biol.* **1978**, *123*, 35-47.
(34) Sailasuta, N. Anson, F. C.; Gray, H. B. *J. Am. Chem. Soc.* **1979**, *101*, 455-458.
(35) Marchesini, A.; Minelli, M.; Markle, H.; Kroneck, P. M. H. *Eur. J. Biochem.* **1979**, *101*, 77-84.
(36) Peisach, J.; Levine, W. G.; Blumberg, W. E. *J. Biol. Chem.* **1967**, *242*, 2847-2858.
(37) Model studies are still required to evaluate the ligand field and charge-transfer contributions of the disulfide ligand.
(38) Dooley, D. M.; Rawlings, J.; Dawson, J. H.; Stephens, P. J.; Andrēasson L.-E.; Malmstrōm, B. G.; Gray, H. B. *J. Am. Chem. Soc.* **1979**, *101*, 5038-5046.
(39) Reinhammar, B. R. M *Biochim. Biophys. Acta* **1972**, *275*, 245-259.